Procedia Engineering

Volume 143, 2016, Pages 1152–1159

Advances in Transportation Geotechnics 3 . The 3rd International Conference on Transportation Geotechnics (ICTG 2016)

Investigation into Impact of Train Speed for Behavior of Ballasted Railway Track Foundations

Md. Abu Sayeed[1*] and Mohamed A. Shahin[2]

[1]*PhD Candidate, Department of Civil Engineering, Curtin University, WA 6845, Australia*

[2]*Associate Professor, Department of Civil Engineering, Curtin University, WA 6845, Australia*

sayeed.ce00@yahoo.com, M.Shahin@curtin.edu.au

Abstract

Traffic congestion of highways in many countries around the world has led railways to become the most popular means of public transportation, which increased the demand for faster and heavier trains. High-speed trains and heavy train loads are normally accompanied with strong vibrations in the track-ground system, which increases the risk of train derailment and track damages. Therefore, to allow for safer and reliable operation of high-speed trains, an investigation into the behavior of ballasted railway track foundations subjected to train moving loads at various speeds is a subject of prime importance in design of railway tracks. In the current study, sophisticated three dimensional (3D) finite elements (FE) numerical modelling was developed to investigate the impact of train speed on the dynamic response of track-ground system. In addition, some factors of the track-ground system affecting the critical speed including the modulus and thickness of track subgrade and ballast materials, and amplitude of train loading were investigated. The results were analyzed and presented, and their practical implications were discussed.

Keywords: Ballasted railway track, Critical speed, Dynamic amplification factor, Finite element numerical modelling, High-speed trains

1 Introduction

Development of railway networks for high-speed trains (HST) is rapidly growing in many countries around the world, to meet the increasing demand for faster transportation. For instance, the Japanese railways authority has constructed the *Shinkansen* HST network 4,072 km long for trains running at a speed of 320 km/h. Recently, using the magnetic levitation technology, the Japanese bullet train broke the world train speed record in a test conducted in 2015 for a train running at a blazing speed of 603 km/h. On the other hand, China has the world largest HST network, which is about 16,000 km long, and

* Corresponding author. Mobile: +61404214238.

Selection and peer-review under responsibility of the Scientific Programme Committee of ICTG 2016

doi:10.1016/j.proeng.2016.06.131

the Chinese railway authority expects that train speed in China will increase up to 400 km/h in the near future. As train speed continues to increase, new challenges and problems related to the performance of rail track foundations arise, primarily due to the significant amplification effects of the track-ground vibrations, and high-speed trains often produce extraordinary large vibrations, especially at the critical speed (i.e. the speed that creates a resonant-like problem) (Alves Costa et al., 2015; Kaynia et al., 2000; Krylov, 2001). The increase in vibrations due to high speed trains are not only a possible source of detrimental environmental effect and human disturbance, but also increases the risk of several train operation issues, including the train safety, degradation or deformation of track foundations, fatigue failure of rails and interruption of train power supply (Kaynia et al., 2000). Therefore, an investigation into the behavior of ballasted railway track under different train speeds has become a key research issue, for avoiding the track resonance and reducing associated possible vibrations.

Problems associated with much soil vibrations due to the dynamic response of moving loads on a surface of an elastic medium has been a subject of research of theoretical basis (e.g. Dieterman and Metrikine, 1997). However, failure in operating the X-2000 passenger HST at Ledsgard site at the West Coast Line between Goteborg and Malmo brought the problem of the impact of high-speed trains to the attention of engineering practices. Subsequently, various formulations including analytical approaches (e.g. Sheng et al., 2004), boundary element models (BEM) (e.g. Andersen and Nielsen, 2003), finite element methods (FEM) (e.g. El Kacimi et al., 2013), and 2.5D FEM-BEM (e.g. Bian et al., 2014) have been proposed for predictions of train-induced ground vibrations. However, to investigate the effect of train speed on track behavior and performance, most available studies considered a single cyclic or moving point (or surface) load rather than a true (dynamic) train moving loads. The assumption of a single cyclic or moving wheel load is highly questionable, as the amount of dynamic amplification and critical speed depend on the wavelength of the site and the distance between the axles and bogies of the car, hence, the role of frequency arises (Kaynia et al., 2000). Therefore, the actual train geometry and magnitude of individual axle load need to be accounted for in the analysis of the effect of train speed.

In the current study, an advanced three-dimensional (3D) finite element (FE) numerical model which was previously established by the authors (Sayeed and Shahin, 2015; Sayeed and Shahin, 2016) was used to investigate the dynamic response of the track-ground system subjected to train moving loads at different speeds, including the subcritical, critical and supercritical. In addition, some factors affecting the critical speed of train, including the modulus and thickness of track subgrade and ballast materials, and amplitude of train loading were investigated. The obtained results were analysed and presented, and their practical implications discussed.

2 Numerical Modelling of Railway Track Foundations

In this study, the dynamic response of railway track foundations subjected to train moving loads at different train speeds was investigated through an advanced 3D FE numerical modelling using the commercial software package Midas-GTS (MIDAS IT. Co. Ltd., 2013). In this section, the FE modelling and simulations are briefly described.

2.1 Finite Element Model

The 3D FE model developed in the current study is depicted in Fig. 1. The track dimensions considered were 80 m long, 36 m wide and 15 m high. The rail was modelled using one-dimensional (1D) *I*-beam section running across the track length. A *UIC*-60 section was assumed for the rail, which was fixed to the sleepers by rail pads that were characterized by an elastic link (spring-like) element of stiffness equal to 100 MN/m. All other track components (i.e. sleeper, ballast and subgrade) were characterized using 3D solid elements. A total of 133 sleepers were placed along the rail at 0.6 m spacing. The rail, sleepers and subgrade were modelled as elastic materials, whereas the ballast was

modelled as an elastoplastic Mohr-Coulomb material. The properties of all model materials are summarized in Table 1.

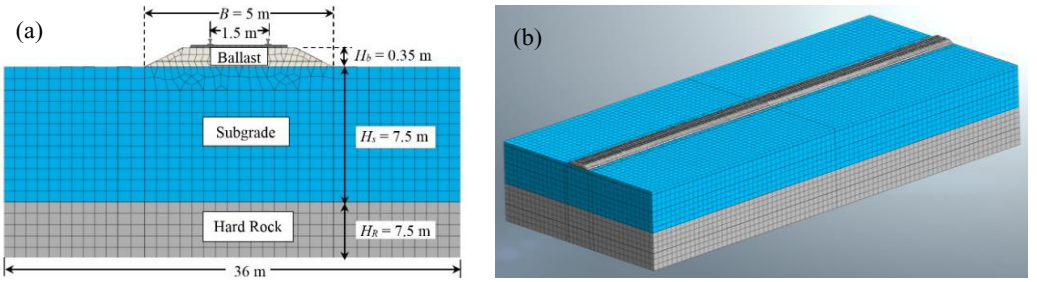

Fig. 1. Three dimensional FE model of track-ground system (a) cross-section of the model (not to scale); (b) 3D view of the model.

Material	Dynamic modulus, E (MPa)	Poisson's ratio, ν	Unit weight, γ (kN/m^3)	Cohession, C (kPa)	Friction angle, ϕ^o	Shear wave veloocy, C_s (m/s)	Rayleigh wave veloocy, C_R (m/s)
Rail	210000	0.30	76.50	–	–	–	–
Sleeper	30000	0.20	20.15	–	–	–	–
Ballast	300	0.30	18.64	0	50	246	229
Subgrade	60	0.33	17.00	–	–	114	106
Hard Rock	500	0.30	18.64	–	–	318	295

Table 1. Material properties used in the FE model.

In FE dynamic analyses, the finite element size, model boundaries and time step have to be selected carefully to ensure the accuracy of results (Galavi and Brinkgreve, 2014). In general, the element size of the FE model was estimated based on the smallest wave-length that allows the high-frequency motion to be simulated correctly. Accordingly, the sizes of the 3D FE model components used in the current study were taken as: 0.167 m × 0.137 m × 0.2 m; 0.2 m × 0.2 m × 0.2 m; and 0.6 m × 0.6 m × 0.6 m for the sleepers, ballast and subgrade, respectively. Hence, the track FE mesh consisted of 326,000 elements. The vertical boundaries of the model were connected to viscous dampers to absorb the incident *S*- and *P*- waves, and to represent infinite boundary conditions (Kouroussis et al., 2011). The nodes at the bottom boundary were fixed in every direction to simulate bedrock. The material damping of the FE model was characterized by the mass and stiffness proportional coefficients, normally referred to as Rayleigh damping, which is commonly used in the dynamic analyses.

2.2 Simulations of Train Moving load

The train geometry and standard axle loads used in the FE numerical modelling were for the X-2000 HST (Alves Costa et al., 2010), as shown in Fig. 2. The train moving loads were modelled in accordance with Araújo (2011) in which the rail FE nodes, which are rigidly connected to the sleepers via pads, were subjected to a wheel load (denoted as *loading nodes*) whose value changes in time (note that the spacing between any two *loading nodes* is 0.6 m). As schematically shown in Fig. 3, the train moving loads can be thought of as triangular pulses distributed among three nodes. The wheel load, F, at one certain *loading node*, N+1, increases once the wheel leaves node N, reaching a peak value when the wheel is directly above node N+1, then finally decreasing back to zero when the wheel reaches the next node N+2. As a result, the triangular pulse moves from one node to another by a time interval equal to the spacing of the loading nodes divided by the speed, c, of the moving loads. In this fashion, a series of train wheels was considered to be moving along the track. During simulation of the moving loads, the time step was chosen based on the well-known Courant-Friedrichs-Lewy condition (Galavi and Brinkgreve, 2014).

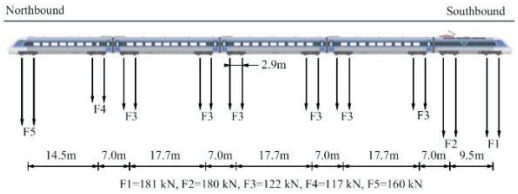

Fig. 2. Geometry and axle load of the X-2000 HST (Alves Costa et al., 2010).

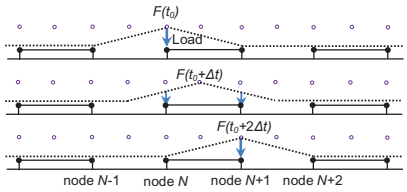

Fig. 3. Simulation of moving loads (Araújo, 2011).

3 Influence of Train Speed

As mentioned earlier, train speed is a major important factor that influences track performance. In this section, the effect of train speed is investigated including the critical speed (i.e. the train speed at which the dynamic response of railway track and surrounding ground are intensely amplified and large vibrations occurred due to resonance), subcritical speed (i.e. speed less than the critical speed) and supercritical speed (i.e. speed higher than the critical speed). The sleeper downward and upward deflections versus the train speed are depicted in Fig. 4. It can be seen that the sleeper deflection generally increases with the increase in the train speed, reaching its maximum value at the critical speed, before it decreases with further increase in the train speed. As can be seen, the critical speed was found to be higher than both the Rayleigh wave (C_R) and shear wave velocities (C_s) of the top subgrade soil overlying the hard rock (the critical speed ≈ 175 m/s versus C_R = 106 m/s and C_s = 114 m/s of the subgrade soil). This result suggests that the critical speed is not always equal to the Rayleigh wave velocity of the top subgrade medium as sometimes thought, and this can be attributed to the existence of the bottom hard rock layer, in which C_R = 295 m/s. This behavior confirms good consistency in the qualitative sense with the results reported by Bian et al. (2014) and Alves Costa et al. (2015). It can also be seen that the effect of train speed on the sleeper upward and downward deflections is negligible for train speed lower than 30% of the critical speed, and the dynamic effects commence after that level of train speed. However, it can be observed that the sleeper deflection increases sharply when the train speed passes around 75% of the critical speed and maintains the same trend until it reaches the critical speed. Therefore, based on the above results, a train speed value equivalent to about 75% of the critical speed may be assumed as the practical speed limit for ballasted railway tracks.

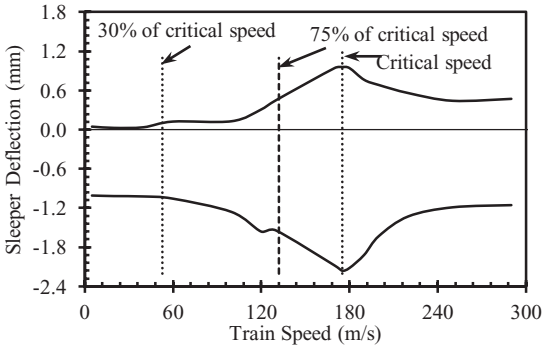

Fig. 4. Effect of train speed on sleeper deflection.

In Fig. 5, the time-history of the sleeper deflection response is presented for three typical speeds, including the subcritical speed (100 m/s), critical speed (175 m/s) and supercritical speed (250 m/s). To compare the track dynamic response of railway track to the three selected train speeds, they were all plotted along a common space axis, converted from the time axis, t, through multiplication by the train

speed, c. It can be seen from Fig. 5 that larger sleeper deflections occur at the critical train speed (175 m/s) than at the other two train speeds (100 m/s and 250 m/s). It can also be seen that for the subcritical train speed (100 m/s), the peaks of sleeper deflections appear at the moment of passage of the respective axle load for the point under consideration. However, for higher train speeds (i.e. critical and supercritical speed), the contribution of the four axle loads (adjacent two bogies) superimposes to give rise to almost one predominant peak, and the track oscillates after the train passage. This behavior agrees reasonably well with the previous published simulated response (Kaynia et al., 2000).

Fig. 6 presents the ground vibrations in terms of the vertical displacements of ground surface from the track center to the neighboring ground, for the three different train speeds considered. It can be seen that the critical speed (175 m/s) provides the highest amplitude of ground vibrations compared to the subcritical (100 m/s) and supercritical (250 m/s). It can also be seen that, for any train speed, the peaks of ground vibrations occur at the track center and reduces with the increasing distance from the track center, as would be expected. In addition, it can be observed that the zone from the track center until about 8 m away from the track center experiences a considerable level of ground vibrations, for all train speeds particularly for the critical speed, which could be detrimental for train operations and may also be a possible source of failure for the neighboring structures.

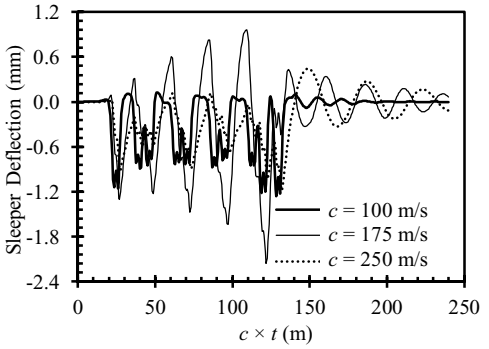

Fig. 5. Time-history dynamic response of sleeper deflection for different train speeds.

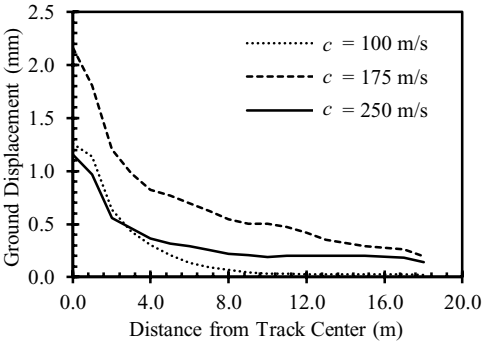

Fig. 6. Variation of ground displacement from the track center at different train speeds.

4 Factors Affecting Critical Speed of Track-ground System

As mentioned earlier, when train speed reaches the critical speed of the track-ground system, large vibrations occur, leading to possible track failure, train derailment and damages to the neighboring structures. To avoid such undesirable scenario, an investigation into the influence of various factors of track-ground system affecting the critical speed was carried out and presented below. For this purpose, the FE model described earlier in Fig. 1 for the X-2000 HST was used.

4.1 Stiffness and Thickness of Track Subgrade

As the wave propagation velocity of any soil medium is highly dependent on its stiffness and thicknesses, the effect of subgrade stiffness (or soil modulus), E_s, and thicknesses, H_s, on the critical speed of train operation was investigated. It is well known that the influence of critical speed is more significant for reduced subgrade stiffness, which means that railway tracks built on soft subgrade usually yield high ground vibrations at low train speed than those founded on stiff subgrade. To investigate the impact of track subgrade stiffness, three different values of track subgrade modulus were considered (i.e. E_s = 15, 60 and 120 MPa). Similarly, the impact of track subgrade thickness was investigated for four different track subgrade thicknesses (i.e. H_s = 5, 7.5, 10 and ∞ m) overlying hard rock.

The impact of track subgrade stiffness and thickness is presented in Fig. 7, in terms of the relationship between the train speed and dynamic amplification factor (DAF). The DAF is defined as the ratio of the maximum dynamic sleeper deflection at a particular train speed to the maximum quasi-static sleeper deflection (i.e. sleeper deflection at a nominal train speed of 5 m/s). It can be seen from Fig. 7 that, for all values of E_s and H_s, the DAF increases with the increase of the train speed until it reaches a peak value corresponding to the critical speed, after which it decreases with further increase in the train speed. Fig. 7(a) shows that, while the critical speed increases with the increase in the track subgrade stiffness, the DAF exhibits an opposite effect. The practical implication of this finding is that the localised ground improvements to spots of soft soil along the rail track can be very beneficial in increasing the critical speed of trains. Fig. 7(b) shows that the magnitude of the critical speed increases with the decrease in the track subgrade thickness. It can also be seen that the critical speed determined for each subgrade thickness is higher than the C_R and C_s of the top subgrade soil overlying the hard rock, except when $H_s = \infty$. This result is in consistent with the findings reported by Alves Costa et al. (2015).

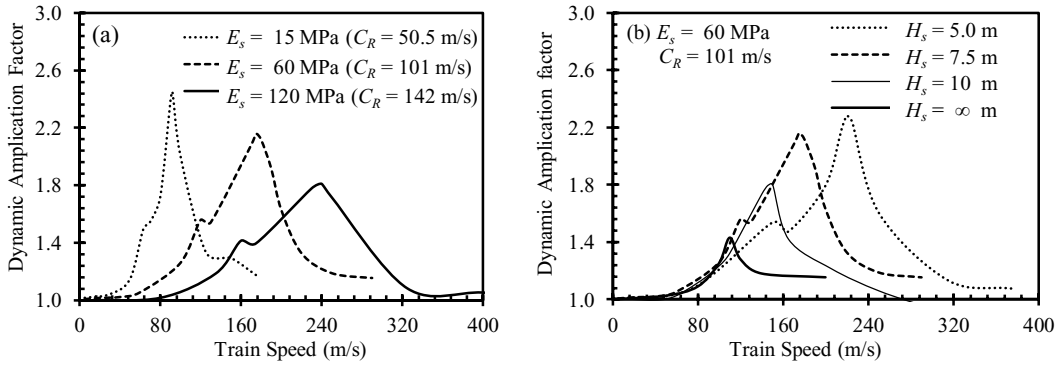

Fig. 7. Evolution of dynamic amplification factor of sleeper downward deflection versus train speed for different: (a) subgrade stiffness; and (b) subgrade thickness.

4.2 Stiffness and Thickness of Ballast Layer

To investigate the influence of ballast stiffness on the critical speed, three different ballast modulus (i.e. E_b = 150, 300 and 500 MPa) were considered. Besides, the influence of ballast thickness was investigated by considering three different ballast thicknesses (i.e. H_b = 0.35, 0.60 and 0.90 m). The relationships between the sleeper deflection and train speed for the different values of ballast stiffness and thickness are shown in Fig. 8. It can be seen that the evolution of DAF of sleeper deflection with

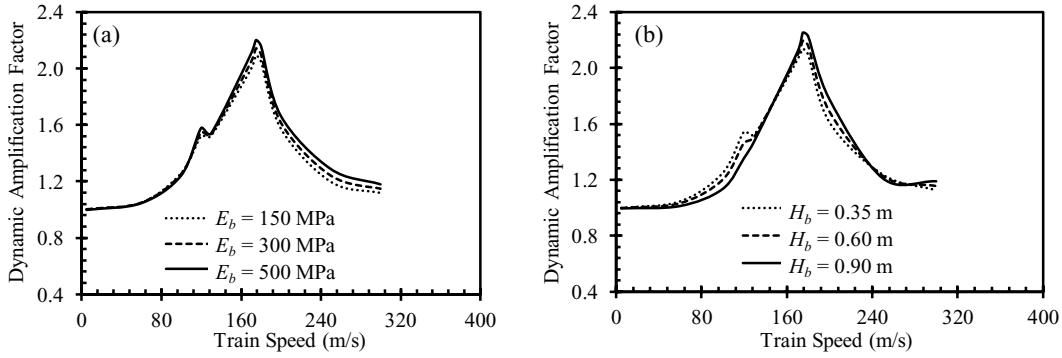

Fig. 8. Evolution of dynamic amplification factor of sleeper downward deflection versus train speed for different: (a) ballast stiffness; and (b) ballast thickness.

the train speed, and the critical speed value are not affected by the ballast stiffness or thickness, which is in contrast to the impact of track subgrade stiffness and thickness, as presented earlier in Fig. 7. This can be attributed to the limited width of the ballast layer compared to the infinite width of the track subgrade, and this prevents the ballast layer contributing to the increase of the Rayleigh wave of the track-ground system, hence, its impact on the critical speed is negligible.

4.3 Amplitude of Train Moving Loads

The influence of amplitude of train moving loads on the critical speed was investigated using three different loading values denoted herein as *standard*, *light* and *heavy*. The standard loading was considered to be equivalent to the axle loads shown in Fig. 2, whereas the light loading was represented as 75% of the standard loading and the heavy loading was represented as 125% of the standard loading. The relationships between the sleeper deflection and train speed for the three considered loading amplitudes are shown in Fig. 9. As predicted, it can be seen that the sleeper deflection increases with the increase in the train loading amplitude, for all train speeds. On the other hand, it can also be seen that the critical speed is almost the same regardless of the train loading amplitude, indicating that the critical speed is independent of the magnitude of train loading.

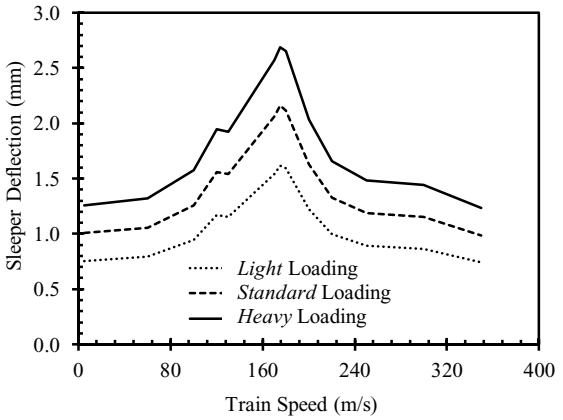

Fig. 9. Time-history dynamic response of sleeper deflection for different train loads.

5 Summary and Conclusions

In this paper, advanced three dimensional finite elements numerical modelling was performed to simulate the dynamic response of ballasted railway track subjected to train moving loads at various train speeds, including the subcritical, critical and supercritical. In addition, the developed FE model was used to carry out further analyses in relation to the critical speed under various conditions of track-ground system. The following conclusions are drawn:

- The evolution of sleeper deflection with train speed indicates that when the train speed exceeds 75% of the critical speed, the amplitude of track dynamic response increases rapidly. Therefore, 75% of the critical speed may be assumed as the practical speed limit of ballasted railway tracks.
- The train speed induces large vibrations at the track center which may extend with less magnitude to a distance equal to 8 m from the track center, which may cause detrimental impact on the track-ground system and nearby structures, and this is especially true for the critical speed.

- As the underlying hard rock has greater stiffness than the subgrade soil, the critical speed was found to be higher than the Rayleigh wave and shear wave velocities of the top subgrade soil.
- The subgrade stiffness and thickness were found to have a significant influence on the dynamic amplification factor (DAF) and critical speed of the track-ground system. The DAF was found to decrease with the increase of both the subgrade stiffness and thickness. On the other hand, the magnitude of the critical speed was found to increase with the increase in the subgrade stiffness and decreases with the increase in the subgrade thickness.
- The ballast stiffness and thicknesses were found to have no influence on DAF and critical speed of the track-ground system.

References

Alves Costa, P., Calcada, R., Silva Cardoso, A., and Bodare, A. (2010). *Influence of soil non-linearity on the dynamic response of high-speed railway tracks*. Soil Dynamics and Earthquake Engineering, 30(4), 221-235.

Alves Costa, P., Colaço, A., Calçada, R., and Cardoso, A. S. (2015). *Critical speed of railway tracks. Detailed and simplified approaches*. Transp Geotec, 2, 30-46.

Andersen, L., and Nielsen, S. R. (2003). *Boundary element analysis of the steady-state response of an elastic half-space to a moving force on its surface*. Engineering Analysis with Boundary Elements, 27(1), 23-38.

Araújo, N. M. F. (2011). *High-speed trains on ballasted railway track: dynamic stress field analysis*, PhD Dissertation, Universidade do Minho.

Bian, X., Cheng, C., Jiang, J., Chen, R., and Chen, Y. (2014). *Numerical analysis of soil vibrations due to trains moving at critical speed*. Acta Geotechnica, 1-14.

Dieterman, H. A., and Metrikine, A. V. (1997). *Steady-state displacements of a beam on an elastic half-space due to a uniformly moving constant load*. European Journal of Mechanics, A/Solids, 16(2), 295-306.

El Kacimi, A., Woodward, P. K., Laghrouche, O., and Medero, G. (2013). *Time domain 3D finite element modelling of train-induced vibration at high speed*. Computers and Structures, 118, 66-73.

Galavi, V., and Brinkgreve, R. B. J. (2014). *Finite element modelling of geotechnical structures subjected to moving loads*. VIII ECNUMGE - Numerical Methods in Geotechnical Engineering, Hicks et al., ed., Taylor and Francis - Balkema, Delft, Netherlands, 235-240.

Kaynia, A. M., Madshus, C., and Zackrisson, P. (2000). *Ground vibration from high-speed trains: prediction and countermeasure*. Journal of Geotechnical and Geoenvironmental Engineering, 126(6), 531-537.

Kouroussis, G., Verlinden, O., and Conti, C. (2011). *Finite-dynamic model for infinite media: corrected solution of viscous boundary efficiency*. Journal of Engineering Mechanics, 137(7), 509-511.

Krylov, V. V. (2001). *Noise and vibration from high-speed trains*. Thomas Telford, London.

MIDAS IT. Co. Ltd. (2013). *Manual of GTS-NX 2013 v1.2: new experience of geotechnical analysis system*. MIDAS Company Limited, South Korea.

Sayeed, M. A., and Shahin, M. A. (2015) *Modelling of ballasted railway track under train moving loads*. 12th Australia New Zealand Conference on Geomechanics, Wellington, New Zealand 1-8.

Sayeed, M. A., and Shahin, M. A. (2016). *Three-dimensional numerical modelling of ballasted railway track foundations for high-speed trains with special reference to critical speed*. Transp Geotec, 6, 55-65.

Sheng, X., Jones, C. J. C., and Thompson, D. J. (2004). *A theoretical study on the influence of the track on train-induced ground vibration*. Journal of Sound and Vibration, 272(3), 909-36.